CHAPTER 1

INTRODUCTION TO THE THESIS

Solids are divided into three major classes that are metals, semimetals and insulators. A metal is a conductor in which electric current flows when an electric field is across it. Application of an electric field across an insulator does not produce current flow. There is a simple criterion to distinguish between the three classes on the basis of the energy-band theory. This criterion rests on the following statement: A band which is completely full carries no current, even in the presence of an electric field. Hence a solid behaves as a metal only when some of the bands are partially occupied. Semiconductors are a group of materials having electrical conductivities intermediate between metals and insulators. The most important property of these materials is that their conductivity can be varied over orders of magnitudes by changes in temperatures, optical excitation, and impurity content.

Semiconductors have been widely studied for a long time (since 1920's). Studies on semiconductor intensified after Shockley, Bardeen, and Brattain invented the transistor in the late 1940's. This invention led to the development of other solid-state devices.

Combination of group II and VI elements produces semiconductors with large band gap. ZnS ($Eg=3.7eV$) [Persson and Zunger, 2003] and $ZnSe$ ($Eg=2.82eV$) [Huang and Ching, 1993] are examples. They have received a lot of attention due to:

(a) Their potential application in optoelectronic devices operating in the visible-light range and as UV photo detectors [Jeon *et al.*, 1992; Kawakamin *et al.*, 1993].

(b) The possibility of having a vanishingly small conduction band offset ΔE_c [Qteish *et al.*, 1995].

In semiconductor alloys, the band gap value and the lattice parameters are among the most important physical parameters. These parameters control the band offset and the mismatching in different devices. The lattice parameter of the ternary alloy AB_xC_{1-x} is well described by Vegard's law, but this is not the case of the band gap value [Van Vechten, 1970].

Energy band gap and electron effective mass as well as their composition dependence are the most critical parameters for band structure calculations of semiconductor alloys. Therefore, an accurate knowledge of these parameters is very important. Unfortunately, there is limited experimental and theoretical information in the literature regarding the electronic band parameters for ZnS_xSe_{1-x} alloys.

Ghatak *et al.*, [2008] presented a relation between the energy band gap Eg and reduced mass μ^* based on the model which was presented by Kane [1957] i.e., the three- band model of Kane. Ghatak and co-workers improved Kane's model and presented a new relation between energy band gap Eg and the ratio (μ^*/m_c), beginning from the Hamiltonian to establish their theory. We believe that the reduced mass μ^* is related to the energy gap Eg. By developing a relationship between the ratio (μ^* /m_c) and unperturbed energy gap Eg_0 from experimental results obtained from the literature a theory for calculating energy gap Eg for ZnS_xSe_{1-x} is established.

1.1 OBJECTIVES

1) To compute using CASTEP the unperturbed energy band gap of ZnS_xSe_{1-x} ($0 \leq x \leq 1$).
2) To develop a theory based on $\vec{k}.\vec{p}$ perturbation theory to predict the band gap for ZnS_xSe_{1-x} ($0 \leq x \leq 1$).
3) To compare predicted energy band gap using Eg_0 obtained from computation using CASTEP with published experimental results.
4) To use the developed theory and formulate the density of states (DOS) for the II–VI materials in the presence of a quantizing magnetic field.

1.2 OUTLINE OF THESIS

Chapter 2 presents a review of energy bands, semiconductor band structures, and the simple theory of band structure by solving the Schrödinger equation are given in section 2.1. In section 2.2 the definition of Brillouin zone and first Brillouin zone will be presented together with the concept of real space and reciprocal lattice vector. In section 2.3 the normal form of energy band and axes of the Brillouin zone of the face centered cubic (fcc), body centered cubic (bcc), simple cubic and hexagonal lattices and the notations used to label the critical points of high symmetry are described. Section 2.4 reviews crystal structures of some ZnS_xSe_{1-x} alloys. The lattice parameters and properties of these compounds will be listed in section 2.7. Sections 2.5, 2.6 review the definitions of effective mass and reduced mass.

In section 2.8 the band gaps for ZnS_xSe_{1-x} $(0 \leq x \leq 1)$ from previous works will be tabled and the main theory of the energy gap for the II-VI materials reported. Sections

2.9, 2.10, 2.11 and 2.12 review the main ideas of Schrödinger equation, perturbation theory, $\vec{k}.\vec{p}$ theory, and the spin-orbit interaction respectively. Section 2.13 reviews the effect of large magnetic field, and section 2.14 reviews the definition of density of states function and the determination of density of states.

Section 2.15 covers the concept of the density functional theory (DFT) and the two fundamental mathematical theorems proven by Hohenberg and Kohn (H-K) (Hohenberg and Kohn, 1964) and the derivations by Kohn and Sham (K-S) [Kohn and Sham, 1965] which are important for the entire field of DFT. The local density approximation (LDA) will be described in subsection 2.15.1, local spin density approximation (LSDA) in subsection 2.15.2 and the generalized gradient approximation (GGA) in subsection 2.15.3. GGA is used in the Cambridge Serial Total Energy Package (CASTEP). The general overview of density functional theory and information on the concepts of charge density, the self-consistent field (SFT) procedure and band structure, are reviewed in section 2.16. Subsection 2.16.1 shows that the wave vectors are reciprocal lattice vectors of the crystal and each electronic function can be written as a sum of plane waves.

In subsection 2.16.2 the exchange-correlation functions such as local LDA, gradient-corrected GGA and fully nonlocal is implemented in CASTEP which are reviewed. Subsection 2.16.3 reviews the concept of pseudopotential applications. Subsection 2.16.4 reviews the idea of the self-consistent electrons minimization of the total energy.

In **Chapter 3** the CASTEP simulation will be used to calculate the electronic-energy band structures and total density of states for ZnS, $ZnS_{0.125}Se_{0.875}$, $ZnS_{0.25}Se_{0.75}$,

$ZnS_{0.3755}Se_{0.625}$, $ZnS_{0.5}Se_{0.5}$, $ZnS_{0.625}Se_{0.375}$, $ZnS_{0.75}Se_{0.25}$, $ZnS_{0.875}Se_{0.125}$, and $ZnSe$. The figures representing the Brillouin zone for each compound will be presented. The energy band gap result for these compounds will be compared with published results from the literature.

In **Chapter 4** the use of $\vec{k}.\vec{p}$ perturbation theory to develop a theory to predict the energy gap for II-VI materials with the effect of spin neglected. The theory is derived in section 4.1. Our contribution to this theory is the incorporation of an empirical relationship that leads to the formulation of a new expression for the energy band equation that can be used to calculate the band gap ZnS_xSe_{1-x}. The energy gap for ZnS_xSe_{1-x} materials is then compared with experimental results given by Abo-Hassan *et al.*, [2005a] and Larach *et al.*, [1957] to examine the suitability of the new equation. Results are plotted in section 4.2.

In **Chapter 5** the $\vec{k}.\vec{p}$ perturbation theory will again be used to develop the theory to calculate the energy gap for II-VI materials but effect of spin is included. Results will again be compared with published results.

In **Chapter 6** the density of states (DOS) of ZnS_xSe_{1-x} is formulated. The effect of magnetic fields on the density of states for II-VI materials will be studied.

In **Chapter 7** results from this work will be discussed and **Chapter 8** concludes the thesis with suggestions for future studies.

CHAPTER 2

LITERATURE REVIEW

2.1 INTRODUCTION

In solid-state physics, the electronic band structure (or simply band structure) of a solid describes the range of energy an electron is "forbidden" or "allowed" to have. Band structure is derived from the diffraction of the quantum mechanical electron waves in a periodic crystal lattice with a specific crystal system and Bravais lattice. The band structure of a material determines several characteristics, in particular the material's electronic and optical properties.

Any solid has a large number of bands. In theory, a solid can have infinitely many bands (just as an atom has infinitely many energy levels). However, all but a few of these bands lie at energies so high that any electron that has attained such energy will escape from the solid. These bands are usually disregarded.

Bands have different widths, depending upon the properties of the atomic orbital from which they arise. Also, allowed bands may overlap, producing (for practical purposes) a single large band. Figure 2.1 illustrates the electronic band structure of typical solid materials. The difference in the type of solids may be attributed to the band gap. In metals there is effectively no band gap and the band gap of insulators are larger than semiconductors.

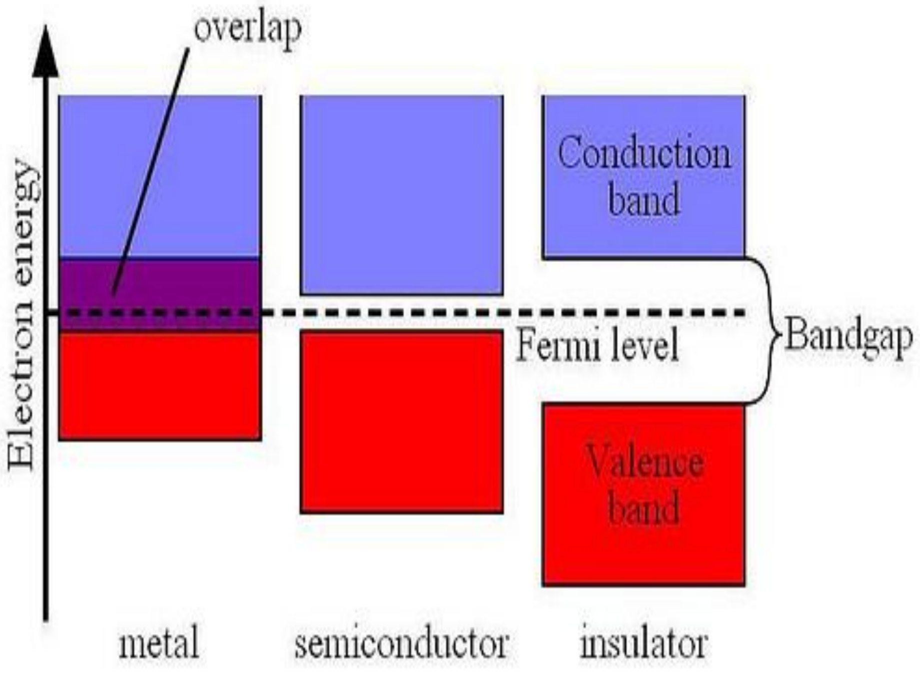

Figure 2.1: Simplified diagram of the electronic band structure of metals, semiconductors, and insulators.

2.2 THE ENERGY BANDS

The failure of the free electron model to explain the dissimilarity between metals, semimetals, semiconductors and insulators has led to the development of theory of band structures in crystals. The atoms in crystals are arranged in a periodic potential which gives the energy bands as shown in Figure 2.2. Electrons are allowed in the bands but forbidden in the gap.

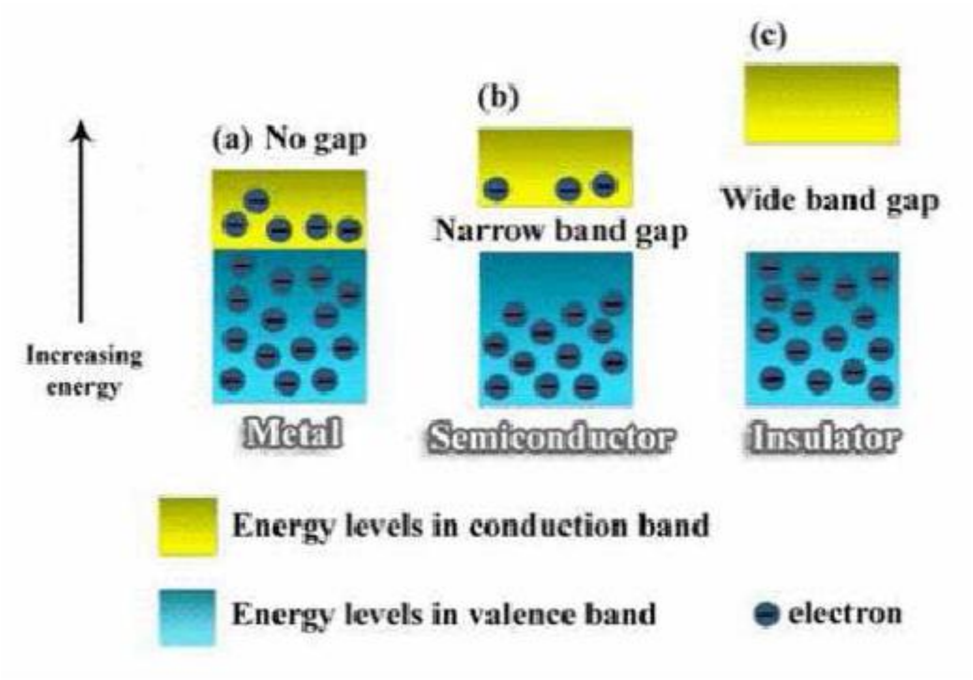

Figure 2.2: Schematic electron occupancy in allowed energy bands for (a) metal, (b) semiconductor and (c) insulator which is showing no gap, narrow and wide band gap respectively. The metal has half filled conduction band, the insulator has no population in the conduction band and the semiconductor has a very small population of electrons [Kittel, 1996]**.**

A semiconductor is a material with a small but nonzero band gap which behaves as an insulator at absolute zero but allows thermal excitation of electrons into its conduction band at temperatures which are below its melting point. In contrast, a material with a large band gap is an insulator. In conductors, the valence and conduction bands may overlap, so they may not have a band gap. The conductivity of intrinsic semiconductors is strongly dependent on the band gap. The only available carrier for conduction is the electrons which have enough thermal energy to be excited across the band gap. Figure 2.3 illustrates the band structure of semiconductors.

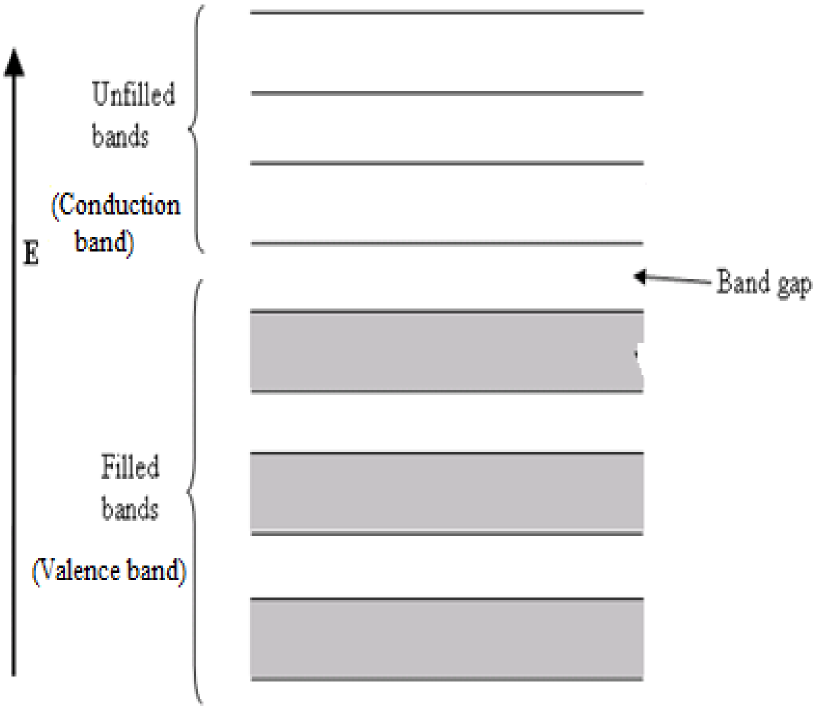

Figure 2.3: Semiconductor band structure.

The band gap energy of semiconductors tends to decrease with increasing temperature as can be understood from Eqn. (2.1). When temperature increases, amplitude of atomic vibrations increases, leading to larger interatomic spacing. The interaction between the lattice phonons and the free electrons and holes will also affect the band gap to a smaller extent. The relationship between band gap energy and temperature can be described by Varshni's empirical expression as given by Vainshtein *et al.*, [1999],

$$Eg(T) = Eg(0) - \frac{\alpha T^2}{T+\beta} \tag{2.1}$$

where T is the temperature, $Eg(0)$ is the magnitude of Eg at zero temperature and α, β are material constants.

In the periodic crystal lattice, the quantum mechanical electron waves occur such that the conduction electron waves interact with the ion cores which results in the formations of the band gaps [Kittel, 1996]. Each crystal consists of infinite bands with different widths and has special characteristic features when a single band overlaps with another band. A discontinuity in energy between the bottommost of the conduction band which is almost unoccupied and the uppermost of the valence band which is almost fully occupied is the energy gap where a particle like wave electron is forbidden from propagating. Current will flow in the crystal only if an electron gets sufficient energy to cross-over the band gap and gets excited to the conduction band. Three major types of materials that we have to concern with are metals, semiconductors, and insulators. If the conduction band is partly filled 50% regardless of temperature, the crystal behaves as a metal. The crystal is an insulator whenever the electrons cannot move under the influence of an electric field to the empty conduction band. The crystal is characterized to be a semiconductor if one or two conduction bands are slightly filled or slightly empty. Therefore, metals have very high conductivity and lower electrical conductivity is found in insulators. The conductivity dependence on temperature of a material is the property that enables semiconductors to conduct current since the conductivity and intrinsic carrier concentration are largely controlled by Eg/k_BT, the ratio of the band gap to thermal energies.

In a regular semiconductor crystal, the band gap is fixed owing to continuous energy states. In a quantum dot crystal, the band gap is size dependent and can be altered to produce a range of energies between the valence band and conduction band. It is also known as quantum confinement effect. Band gaps also depend on pressure. Band gaps can be either direct or indirect, depending on the electronic band structure.

Ghatak *et al.,* [2008] studied theoretically the electron energy spectrum and the photoemission from ternary and quaternary materials in the presence of light waves, whose unperturbed energy band structures are defined by the three-band model of Kane. They expressed the band gap of semiconductors by the expression [Chakraborty *et al*., 2007; Ghatak *et al*., 2007]

$$Eg = Eg_0\left(1+\left(\frac{2m_c}{\mu^*}\right)\frac{E\left(1+\alpha E\right)}{Eg_0}\right)^{\frac{1}{2}} \tag{2.2}$$

where m_c is the effective electron mass at the edge of the conduction band, and μ^* is the reduced mass and is given by

$$\frac{1}{\mu^*}=\frac{1}{m_c}+\frac{1}{m_v} \tag{2.3}$$

m_v is the effective mass of the heavy hole at the top of the valence band , Eg_0 is the unperturbed band gap, and $\alpha=1/Eg_0$.

These authors have in the past several years studied the Boltzmann transport equation and have introduced new insights for experiments in the presence of external photo excitation.

Afia *et al.,* [2005], reported that the energy band gaps and electron effective mass as well as their composition dependence are the most critical parameters for band structure calculations of semiconductor alloys, therefore, an accurate knowledge of these parameters is very important. In their computation they declare that the band gap variation versus sulfur concentration shows two different behaviors: clear diminution of gap energy for low concentrations, and quasi linear behavior with a small bowing for large values of x.

The theory of band structure in crystals is simplified with the consideration of only one electron in a periodic crystal lattice. Actually, the crystal always has been a many- electron problem. In fact, the crystals will have imperfections, voids, and dangling bonds and are not perfectly periodic. The solution of Schrödinger's equation [Schrödinger, 1926] can be expressed as Bloch waves

$$\Psi_i\left(\vec{r}\right)=\psi_i\left(\vec{r}\right)e^{i\vec{k}.\vec{r}} \qquad (2.4)$$

in which $\psi_i\left(\vec{r}\right)$ is periodic in $\vec{r}$ with the periodicity of the potential in Eqn. (2.4) characterized by the wave number k and the energy of a state ψ_i. An energy band results from the relation between energy and wave number.

2.3 BRILLOUIN ZONE

Information relating to the energy band structure is usually presented by plotting the energy of the electron E for values of the wave vector $\vec{k}$, limited to within the first Brillouin zone. The concept of a Brillouin zone [Callaway, 1958] was first developed by Léon Brillouin (1889-1969), a French physicist. During his work on the propagation of electron waves in a crystal lattice, he introduced the concept of Brillouin zone in 1930. A Brillouin zone is defined as a Wigner-Seitz primitive cell [Wigner and Seitz, 1933] in the reciprocal lattice. The first Brillouin zone is the smallest volume entirely enclosed by planes that are the perpendicular bisectors of the reciprocal lattice vectors drawn from the origin. The concept of Brillouin zone is particularly important in the consideration of the electronic structure of solids. There are also second, third, *etc*., Brillouin zones, corresponding to a sequence of disjoint regions (all with the same volume) at increasing distances from the origin, but these are rarely used. As a result, the first Brillouin zone is often called simply the Brillouin zone. The region in *k*-space (here an imaginary plane whose rectangular coordinates are k_x and k_y) that low-k electrons can occupy without being diffracted is called first Brillouin Zone, shown in Figure 2.4. The second Brillouin zone is also shown; it contains electrons with *k* values form π/a to 2π/a for electrons moving in the ±x and ±y directions, with the possible range of *k* values narrowing as the diagonal directions are approached.

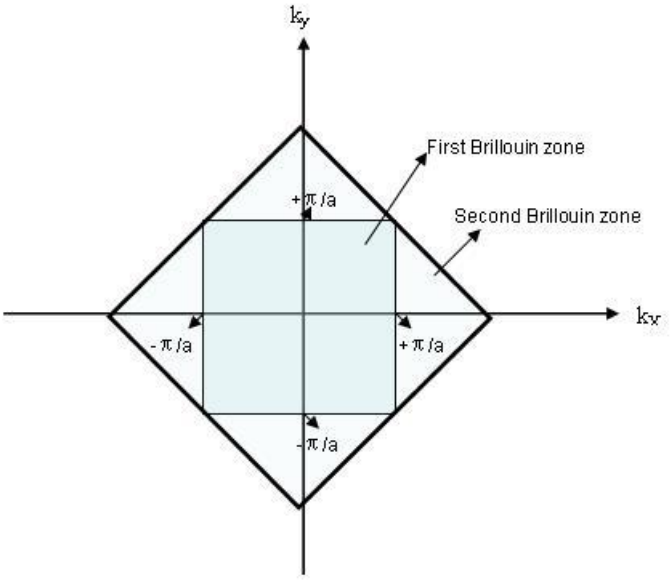

Figure 2.4: The first and second Brillouin zones of a two-dimensional square lattice [Kittel, 1996].

The calculation of the minimum energy of *k* points in the Brillouin zone has to converge for a given Bravais lattice [Sholl and Steckel, 2009]. The Bloch theorem will satisfy the concepts associated with reciprocal space. The periodically repeated cell in space is defined by the lattice vectors a_1, a_2 and a_3. The space of vectors, *r* and *k* are real space and reciprocal space (or simply *k* space) respectively. Three vectors, b_1, b_2 and b_3 that define position in reciprocal space are called the reciprocal lattice vectors just as for lattice vectors a_1, a_2 and a_3 in real space. The expressions are defined so that $a_i.b_j = 2\pi$ if $i=j$ and 0 otherwise as shown in Eqn. (2.5),

$$b_1 = 2\pi \frac{a_2 \times a_3}{a_1.(a_2 \times a_3)},\ b_2 = 2\pi \frac{a_3 \times a_1}{a_2.(a_3 \times a_1)},\ b_3 = 2\pi \frac{a_1 \times a_2}{a_3.(a_1 \times a_2)} \qquad (2.5)$$

The lattice and the reciprocal lattice vectors both define cubes for the former with side length of a and the latter with side length of $2\pi/a$. The real space is the feature of the simplest crystal structure for the face-centered cubic and hexagonal close-packed materials and has been discussed in detail in Kittel [1996] and Sholl and Steckel [2009]. The real space concept describes the primitive cell for the simple cubic material and uses one atom per supercell but eight atoms per supercell is used in the reciprocal space is shown in Figure 2.5.

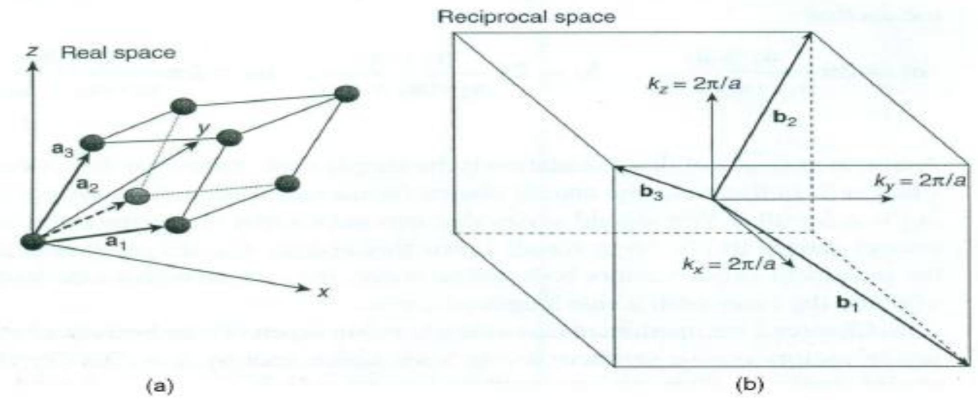

Figure 2.5: The lattice vectors for fcc primitive cell of (a) real space where atoms is represented by circles and (b) reciprocal space with basis vectors shown inside a cube with side length 17/4a centered at the origin [Sholl and Steckel, 2009].

The concepts of real space and reciprocal lattice vector are then considered by the well-known Wigner-Seitz cell in Bravais lattice. The primitive cell that is minimal in terms of volume can be made more precise and also easily defines the reciprocal lattice vectors. The Brillouin zone plays a central role in the band theory of the materials which will be discussed in the next section. We note that the volume of Brillouin zone, V_{BZ} is [Kittel, 1996],

$$V_{BZ} = \frac{(2\pi)^3}{V_{cell}} \tag{2.6}$$

where the V_{cell} is the volume of the primitive cell in real space defined by Wigner-Seitz construction. The integral expression in k space that reduces a great deal of work in DFT calculations is defined in reciprocal space and the integral is performed only over the possible values of k in the Brillouin zone, (Eqn. 2.7), [Kittel, 1996]

$$\bar{g} = \frac{V_{cell}}{(2\pi)^3} \int_{BZ} g(k) d(k) \tag{2.7}$$

2.4 NORMAL FORM OF AN ENERGY BAND

A standard form for a particular band is defined for the reason of strong dependency on the potential by the relation of the various bands to each other. It may be a useful concept in metals but somewhat less in semiconductors. In an empty lattice, the corresponding free electron band can be defined as *s*, *p* and *d* bands at symmetry points of the Brillouin zone determined in the expansion of the wave function by the lowest spherical harmonic [Bell, 1954]. There is exactly one independent value of k that contributes to each energy band. If two independent orientations of the electron spin are taken into account, in each energy band there are $2N$ independent orbitals where, N is the number of primitive cells. A band with half filled electrons or it can be exactly filled if contribution of one or two valence electron in each primitive cell by a single atom respectively. For which k =0 known as Γ type is that of the lowest level would be formed from plane wave in an "empty" lattice of the body-centered cubic type. However, the symmetry of this minimum is different in the body-centered and face-centered cubic as shown in Figure. 2.6. The notations are described and tabulated in Table 2.1.

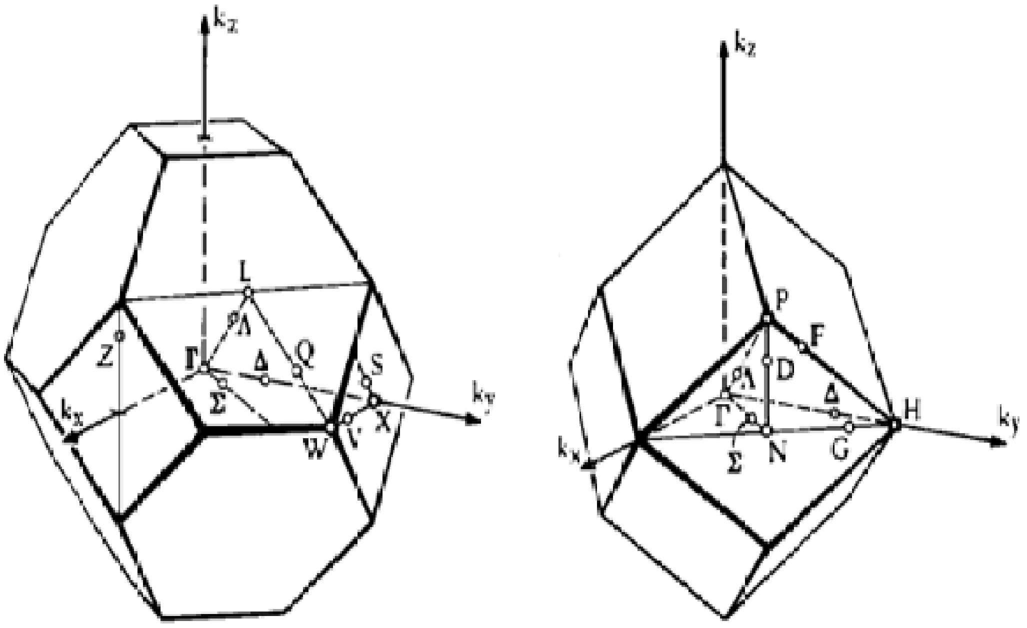

FACE CENTERED CUBIC

BODY CENTERED CUBIC

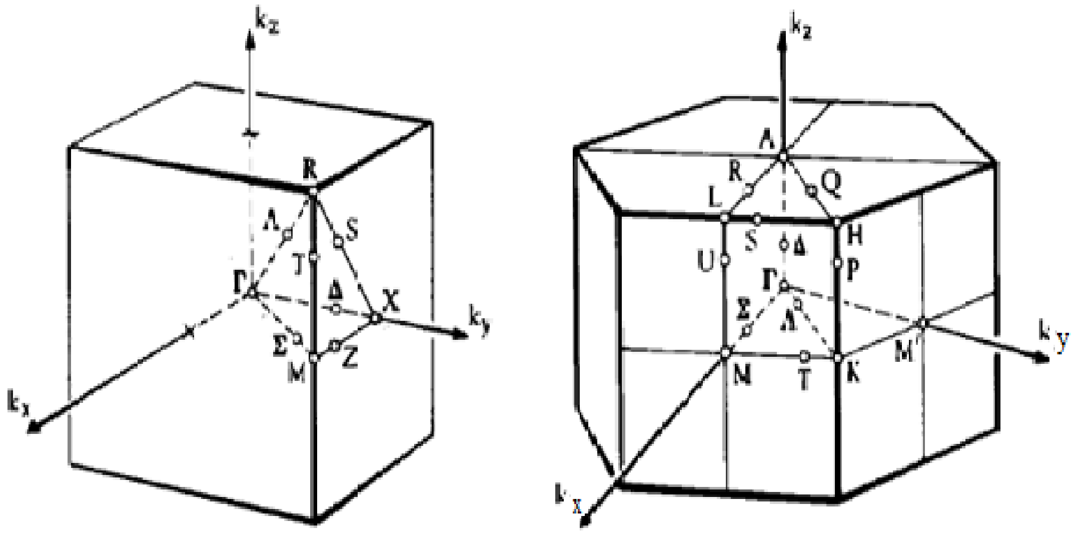

SIMPLE CUBIC

HEXAGONAL

Figure 2.6: Standard labels of the symmetry and axes of the Brillouin zone of the face centered cubic (fcc), body centered cubic (bcc), simple cubic and hexagonal lattices where Γ is the zone center(k=o on Γ point) [Kittel, 1996].

Table 2.1: The notations, used to label the critical points of the symmetry and axes of the Brillouin zone.

Symbol	Description
Γ	Center of the Brillouin zone
Simple cubic	
M	Center of an edge
R	Corner point (intersected three edges)
X	Center of a face
Face-centered cubic	
K	Middle of an edge joining two hexagonal faces
L	Center of a hexagonal face
U	Middle of an edge joining a hexagonal and a square face
W	Corner point
X	Center of a square face
Body-centered cubic	
H	Corner point joining four edges
N	Center of a face
P	Corner point joining three edges
Hexagonal	
A	Center of a hexagonal face
H	Corner point
K	Middle of an edge joining two rectangular faces

2.5 ZnS_xSe_{1-x} $(0 \leq x \leq 1)$ AS II-VI COMPOUNDS CRYSTAL STRUCTURE

Almost all compounds of the II-VI type crystallize in such a manner that each atom of one element is located at the center of a regular tetrahedron, the apices of which are occupied by atoms of the other element. Two possible structures can be formed from such tetrahedral: the sphalerite (cubic type) and the wurtzite (hexagonal) type. The sphalerite structure is very similar to the structure of diamond, but it differs from the latter by the alternation of atoms of two different elements. In the sphalerite structure, the atoms of one element are located at the sites of a fcc lattice, while the atoms of the second element occupy the centers of four (out of a total of eight) small cubes (Figure 2.7 and Figure 2.8). The space group is F43m. Figure 2.9 shows the wurtzite structure. Its space group is P63mc.

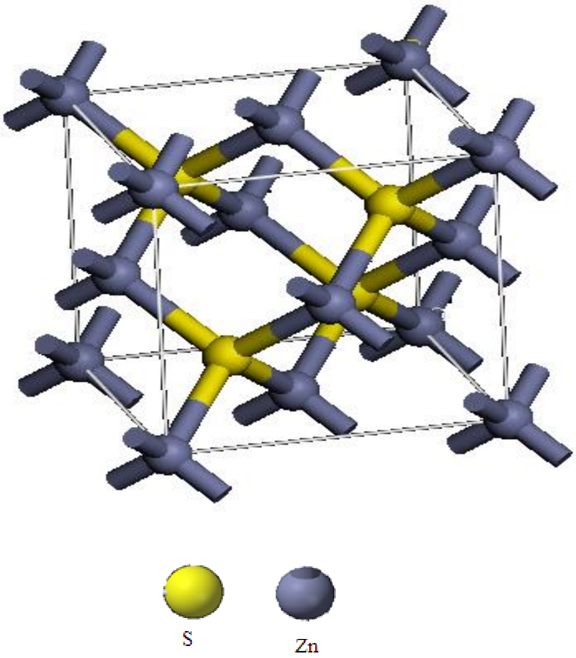

Figure 2.7: Crystal structure of sphalerite for *ZnS* with space group F-43M (TD-2). The lattice parameters for ZnS sphalerite crystal structure are a=5.41 Å [Aswegen and Verleger, 1960].

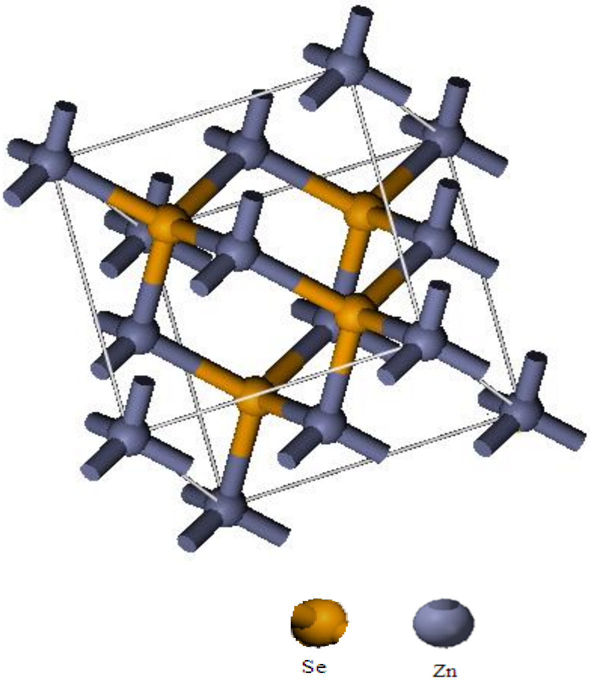

Figure 2.8: Crystal structure of sphalerite for *ZnSe* with space group F-43M (TD-2). The lattice parameter for ZnSe sphalerite crystal structure a=5.6686±0.006 $\overset{0}{\mathrm{A}}$ [Goryunova and Fedorova, 1959].

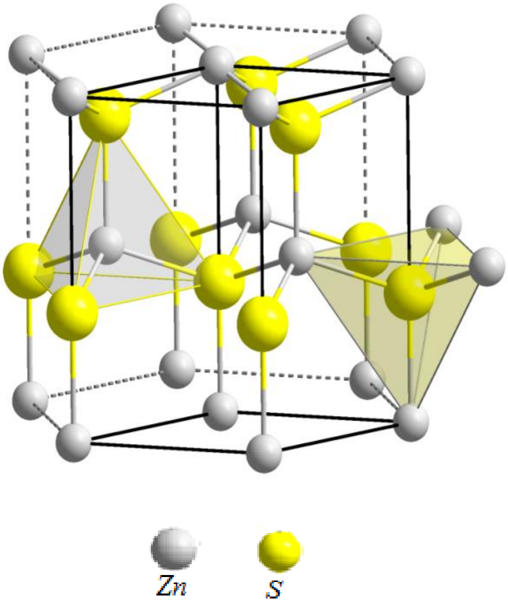

Figure 2.9: Crystal structure of wurtzite for *ZnS* with space group P63mc. The lattice parameter for wurtzite crystal structure a=3.82 $\overset{0}{\mathrm{A}}$ **, c=6.26** $\overset{0}{\mathrm{A}}$ [Hansen and Andreko, 1968], **for ZnSe the lattice parameter in case of wurtzite crystal structure are a=4.01±0.02** $\overset{0}{\mathrm{A}}$ **, c=6.54±0.02** $\overset{0}{\mathrm{A}}$ [Pashinkin *et al*., 1960; Goryunova and Fedorova, 1959]**.**

Figures 2.10 shows the sphalerite crystal structure with space group P-42M (D2D-1). Figures 2.11 and 2.12 show the sphalerire crystal structure with space group P-4M2

(D2D-5), while figures 2.13 and 2.14 show the sphalerite crystal structure with space group CMM2 (C2V-11).

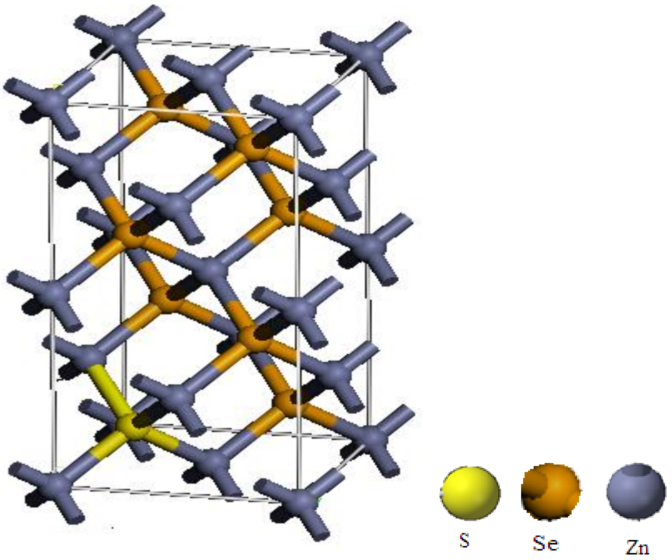

Figure 2.10: Crystal structure of sphalerite for $ZnS_{0.125}Se_{0.875}$ with space group P-42M (D2D-1) and lattice parameter a=b=5.4093 $\overset{0}{A}$, c=10.8186 $\overset{0}{A}$ [CASTEP simulation]**.**

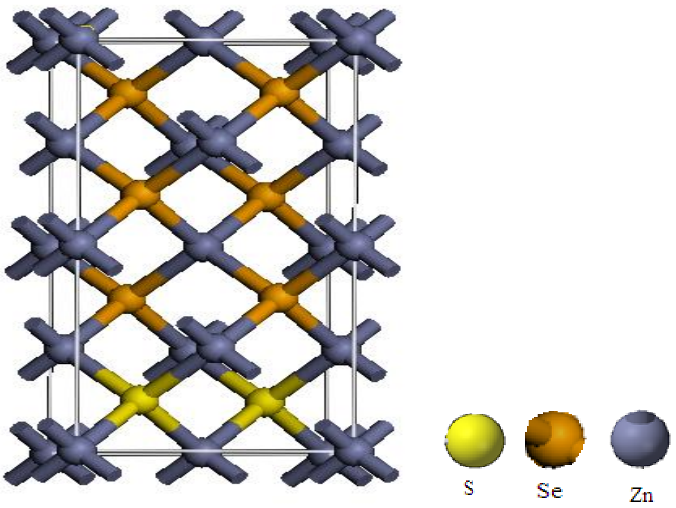

Figure 2.11: Crystal structure of sphalerite for $ZnS_{0.25}Se_{0.75}$ with space group P-4M2 (D2D-5) and lattice parameter a=b=5.4093 $\overset{0}{A}$, c=10.8186 $\overset{0}{A}$ [CASTEP simulation]**.**

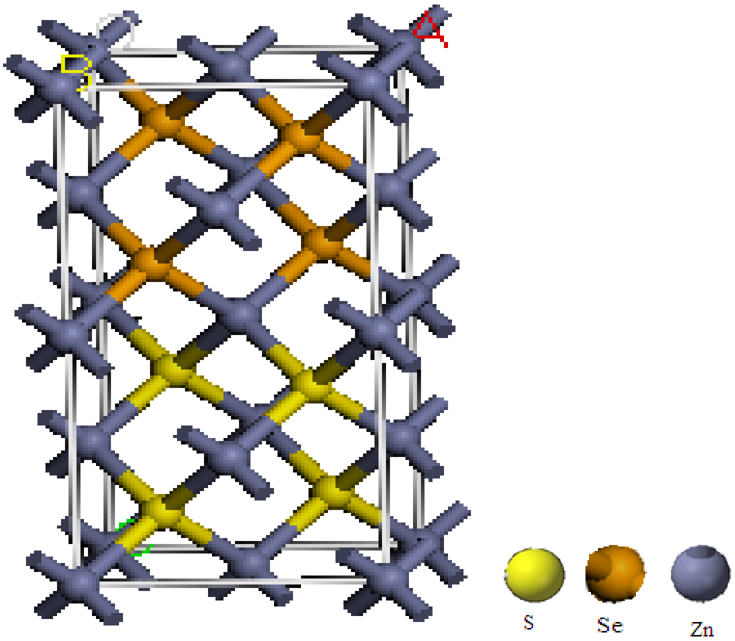

Figure 2.12: Crystal structure of sphalerite for $ZnS_{0.5}\ Se_{0.5}$ with space group P-4M2 (D2D-5) and lattice parameter a=b=5.4093 Å, c=10.8186 Å [CASTEP simulation]**.**

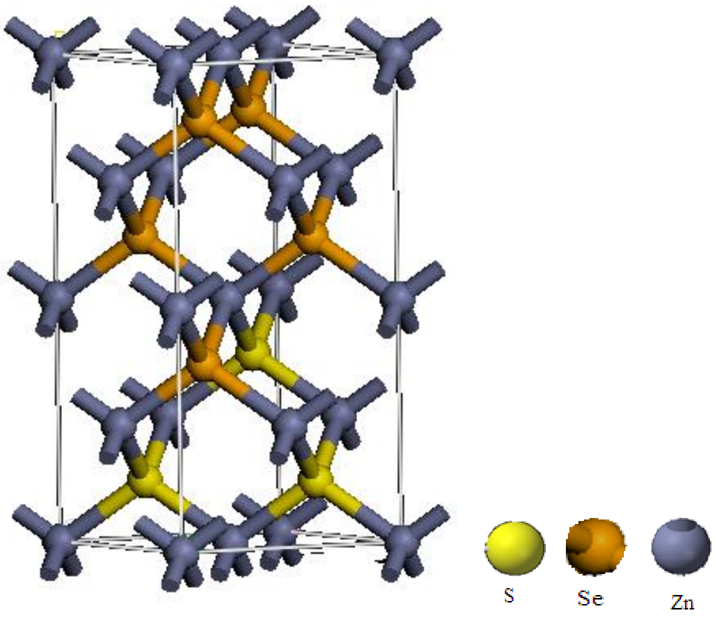

Figure 2.13: Crystal structure of sphalerite for $ZnS_{0.375}\ Se_{0.625}$ with space group CMM2 (C2V-11) and lattice parameter a=b=5.4093 Å, c=10.8186 Å [CASTEP simulation]**.**

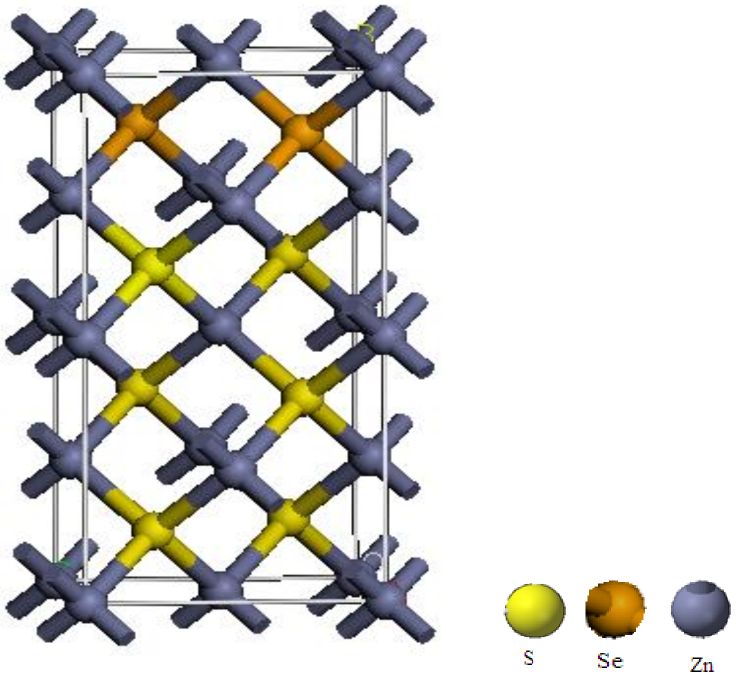

Figure 2.14: Crystal structure of sphalerite for $ZnS_{0.75}\,Se_{0.25}$ with space group CMME (C2V-11) and lattice parameter a=b=5.4093 $\overset{0}{A}$, c=10.8186 $\overset{0}{A}$ [CASTEP simulation]**.**

The basic difference between the sphalerite and wurtzite crystal structures is in the positions of atoms in the third coordination sphere, because the distances from a given atom to its neighbors in that sphere are shorter in the wurtzite structure than in the sphalerite structure [Birman, 1958]. Therefore, we may expect the compound with a large difference between the electro-negativities of the constituent elements usually have the wurtzite structure, that is for *ZnS* and *ZnSe* crystal structure.

At room temperature, the application of high pressures induces transitions in chalcogenides of the zinc subgroup. The pressure at which such phase transitions occur and the crystal structures of the high-pressure phases: for *ZnS* sphalerite crystal structure at pressure 240-250 kbar the crystal structure becomes CsCl crystal structure, and for *ZnSe* sphalerite crystal structure at pressure 165kbar becomes CsCl crystal structure [Drickamer, 1963]. Note that the caesium chloride CsCl structure adopts a primitive cubic lattice with a two atom basis, where both atoms have eightfold coordinates. The chloride atoms lie upon the lattice points at the edges of the cube, while the caesium atoms lie in the holes in the center of the cubes as shown in Figure 2.15.

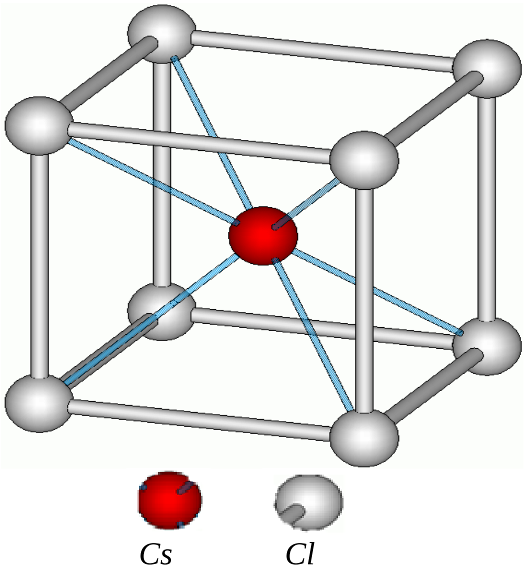

Figure 2.15: ***CsCl* crystal structure** [Slyusarenko, 2008].

2.6 EFFECTIVE MASS

Effective mass is defined by analogy with Newton's second law $F=ma$. Using quantum mechanics it can be shown that for an electron in an external electric field E, the acceleration a_l along coordinate direction l is:

$$a_l = \frac{1}{\hbar^2}\sum_m \frac{\partial^2 \varepsilon(k)}{\partial k_l \partial k_m} q E_m \tag{2.8}$$

where $\hbar = h/2\pi$ is reduced Planck's constant, k is the wave vector (often loosely called momentum since $k = p/\hbar$ for free electrons), ε (k) is the energy as a function of k, or the dispersion relation as it is often called. For a free particle, the dispersion relation is quadratic, and so the effective mass would be constant (and equal to the real mass). In a crystal, the situation is far more complex. The dispersion relation is not even approximately quadratic in the large scale. However, wherever a minimum occurs in the dispersion relation. The minimum can be approximated by a quadratic curve in the small region around that minimum, for example:

$$\frac{1}{\hbar^2}\varepsilon(k) \approx \frac{1}{\hbar^2}\varepsilon(k=0) + \frac{1}{m_x}k_x^2 + \frac{1}{m_y}k_y^2 + \frac{1}{m_z}k_z^2 \tag{2.9}$$

where the minimum is assumed to occur at k=0. In many semiconductors the minimum does not occur at k=0. For example, in silicon the conduction band has six symmetrically located minima along the Δ= [100] symmetry lines in k-space. The constant energy surfaces at these minima are ellipsoids oriented along the k-space axes as shown in Figure 2.16.

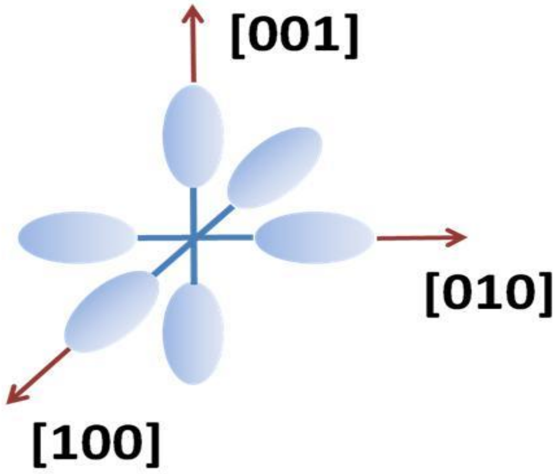

Figure 2.16: Constant energy ellipsoids in silicon near the six conduction band minima. The longitudinal and transverse effective masses are m_l =0.92 m and m_t = 0.19 m with m the free electron mass [Kittel, 1996].

In contrast, the holes at the top of the silicon valence band are classified as *light* and *heavy* and the band energies for the two types are given by a complicated relation [Kittel, 1996]:

$$\varepsilon(k) = Ak^2 \pm \sqrt{B^2k^4 + C^2\left(k_x^2k_y^2 + k_y^2k_z^2 + k_z^2k_x^2\right)} \tag{2.10}$$

leading to what is termed *warped* energy surfaces. Parameters A, B and C are wavevector independent constants. This behavior is introduced here to alert the reader that it is common for carriers to have rather non-parabolic energy-wavevector relations. A simplification can be made, however, for electrons which have energy close to a minimum, and where the effective mass is the same in all directions. The mass can be approximated as a scalar m^* [Kittel, 1996]:

$$m^* = \hbar^2 . \left[\frac{\partial^2 \varepsilon}{\partial k^2} \right]^{-1} \tag{2.11}$$

In energy regions far away from a minimum, the effective mass can be negative or even approach infinity. Effective mass, being generally dependent on direction (with respect to the crystal axes), is a tensor. However, for many calculations the various directions can be averaged out.

2.7 REDUCED MASS

Reduced mass is the "effective" inertial mass appearing in the two-body problem of Newtonian mechanics. This is a quantity with the unit of mass, which allows the two-body problem to be solved as if it were a one-body problem. Note however that the mass determining the gravitational force is *not* reduced. In the computation one mass can be replaced by the reduced mass, if this is compensated by replacing the other mass by the sum of both masses. The reduced mass is frequently denoted by the Greek letter μ.

Given two bodies, one with mass m_1 and the other with mass m_2, the equivalent one-body problem, with the position of one body with respect to the other as the unknown, is that of a single body of mass, the reduced mass:

$$m_{red} = \mu = \frac{1}{\frac{1}{m_1} + \frac{1}{m_2}} = \frac{m_1 m_2}{m_1 + m_2} \tag{2.12}$$

where the force on this mass is given by the force between the two bodies. The reduced mass is always less than or equal to the mass of each body and is half of the harmonic mean of the two masses.

2.8 PHYSICAL PROPERTIES OF THE *ZnS* and *ZnSe* COMPOUNDS

Different research activates have been published on the electronic and optical properties of ZnS_xSe_{1-x} alloys and their applications in optoelectronic and microelectronic devices [Lai *et al.*, 2003]. The ternary compound has many advantages over binary compounds because the lattice constant, band gap and optical properties can be varied by changing the composition.

The electrical properties of some of the *ZnS* and *ZnSe* compounds are given in Table 2.2. The optical value of the forbidden band width is given for these compounds. The temperature and pressure coefficients of the forbidden band width, the effective mass, and the optical and static permittivity are all listed.

Table 2.2: Electrical Properties of *ZnS* and *ZnSe* Compounds.

Compound	Forbidden Band width ΔE (eV) [Hamilto, 1964]	Temperature coefficient forbidden band width.10^4 eV/deg [Aigrain and Balkanski, 1961]	Dependence of ΔE on pressure 10^6 eV/kbar [Aigrain and Balkanski, 1961]	Effective mass [Kröger, 1965]		Permittivity	
				Electrons m_n^*/m_0 [Kröger, 1965]	Holes m_p^*/m_0	High Frequency (optical)	Low Frequency (static)
ZnS (Sphalerite Structure)	3.6	-5.3	5.7	0.25	0.5-1	8	
ZnS (Wurtzite Structure)	—	-3.8 $(97<T<293^0K)$	9				
ZnSe (Sphalerite Structure)	2.7	-7.2 $(90<T<400^0K)$	6	0.15-0.17	0.6	8.1	5.75 [Aven *et al.*, 1961]

The value of the effective mass and of the permittivity at optical frequencies is known for the majority of the II-VI compounds and the static permittivity has been determined just for *ZnSe* compound.

The main physical properties for *ZnS* sphalerite crystal structure have been determined as follows: Debye temperature is 315 K [Aigrain and Balkanski, 1961], compressibility 1.3 $(kbar)^{-1}$ and density 4.09 g/cm^3. For ZnSe sphalerite crystal structure: Debye temperature is 400 K [Aigrain and Balkanski, 1961], compressibility is 2.469$(kbar)^{-1}$ and density is 5.26 g/cm^3.

Most of the investigations on zinc sulfide have been carried out as thin films prepared by vacuum evaporation or on powders subjected to heat treatment. The number of studies of single crystals is very few because it is difficult to prepare such crystals.

The preparation of ZnS_xSe_{1-x} alloys is of interest, since it was realized [Bernard and Zunger, 1987] that compounds with physical properties in the intermediate range to that of ZnS and $ZnSe$ could be obtained. For instance, depending on the amount of the sulphur in the alloy, materials with energy gaps between 2.7 and 3.7 eV, within which there is the major part of the solar radiation, can be prepared.

2.9 BAND GAPS FOR ZnS_xSe_{1-x} $(0 \leq x \leq 1)$

As discussed earlier the II-VI compounds ZnS_xSe_{1-x} may have either the sphalerite or the wurtzite crystal structure or allotropic modifications. ZnS and $ZnSe$ are obtainable in the zinc-blend form at room temperature.

Electron mobility has been studied experimentally as well as theoretically in these materials, and we note that the band gaps for these materials are large as seen in Table 2.3. Nonparabolic effects are not therefore significant. The Γ-point minimum being lowest and the crystal structure being cubic, the effective mass and as a result the electron mobility is isotropic.

Table 2.3: Energy band gaps for ZnS_xSe_{1-x} $(0 \leq x \leq 1)$

ZnS_xSe_{1-x} (*x* values)	**Band gap (eV)**						
	Theoretical			**Experimental**			
	Swarnkar *et al.*, [2009]	Van de Walle [1989]	LCAO Homann *et al.*, [2006]	Larach *et al.*, [1957]	Ebina *et al.*, [1974]	Homann *et al.*, [2006]	Abo Hassan *et al.*, [2005a]
0.00	2.77	2.82	3.00	-	2.72	2.58	-
0.12	-	-	-	2.78	-	-	2.58
0.25	2.99	-	3.18	-	2.85	2.73	-
0.34	-	-	-	2.96	-	-	2.95
0.35	-	-	-	2.99	-	-	2.96
0.37	-	-	-	3.01	-	-	2.96
0.41	-	-	-	3.04	-	-	2.99
0.48	-	-	-	3.10	-	-	3.05
0.50	3.21	-	3.29	-	3.08	2.92	-
0.75	3.47	-	3.47	-	3.34	3.17	-
0.78	-	-	-	3.39	-	-	3.29
0.80	-	-	-	3.41	-	-	3.30
0.82	-	-	-	3.44	-	-	3.35
0.96	-	-	-	3.56	-	-	3.51
0.99	-	-	-	3.59	-	-	3.74
1.00	3.85	3.78	3.68	-	3.70	3.45	-

A few theoretical models have been applied on ternary alloys and the binary compounds. Swarnker *et al.* [2009] have calculated the band gap for ZnS_xSe_{1-x} alloys by employing the Empirical Pseudopotential Method (EPM) within the Modified Virtual Crystal Approximation (MVCA). Homann *et al.* [2006] applied linear combination of atomic orbitals (LCAO) method to report electronic and structural properties of ZnS_xSe_{1-x} alloys over entire composition range. The theory presented by Van de Walle is based on the local -density- functional formalism and the model- solid approach [Van de Walle, 1989]. The model predicts reliable values for the experimentally observed lineups in a wide variety of test cases and can be used to explore which combinations of materials and configurations of the strains will lead to the desired electronic properties.

Only a few experimental studies of the ZnS_xSe_{1-x} alloys are reported. The difficulty posed by miscibility in forming the solid state might probably be the reason for paucity of experimental studies. Homann *et al*. [2006] reported band gap for all compositions applying optical spectroscopy at room temperature. Abo Hassan *et al*. [2005a] used optical transmission measurements to determine various optical constants and properties of ZnS_xSe_{1-x} thin films prepared by electron beam evaporation onto glass substrates at 60^0C. Ebina *et al*. [1974] used reflectivity measurements at room temperature to determine the variation with composition of the lowest gap energy up to 6.4eV at near-normal incidence, using a Shimadzu-40R spectrophotometer double-beam prism-grating type with a reflectivity-measurement attachment of their design. Larach *et al*. [1957] made measurement of diffused transmission on several materials with a Cary recording spectrophotometer, Model 14. Energy gap determinations were made by extrapolations on the recorded curves of optical density (log transmission).

On the computation side, Nacer [2003] investigated the electronic band-structures of the strained-layer *ZnS/ZnSe* (001) superlattices (SLs) using the sp^3s^* tight-binding method, which includes the strain and spin–orbit effects. The SL band-structures are studied versus the biaxial strain, layer thickness, and band offsets. The results suggest that the common-cation II–VI heterojunction exhibit a vanishingly small conduction-band offset (CBO). The results obtain showed that the SL valence-band top state is always a heavy-hole localized within *ZnSe* slabs; whereas the conduction-band edge state (electron) is sensitive to the biaxial strain (or VBO). Nacer [2003] compared experimental data and calculated energy gap obtained using a constant value of valence-band offset (VBO): VBO = 0.78 eV for SLs of *ZnSe* substrate; and VBO = 0.90 eV for free-standing SLs for 10 samples as follows: Super lattice from experimental data for SLs grown on *ZnS*/*ZnSe* substrate are 50/8 (lattice constant $a_0=50\ \overset{0}{A}$ for *ZnS* and $a_0=8\ \overset{0}{A}$ for *ZnSe*) , 50/11, 50/23, 50/37, and 50/54 ($\overset{0}{A}$)and the energy gaps of free-standing super lattices (SLs) results are 3.04, 3.00, 2.92, 2.86, and 2.82 eV respectively.

2.10 SCHRÖDINGER EQUATION

In 1926, Schrödinger established a unified scheme valid for describing both the microscopic and macroscopic universes. The formulation, called wave mechanics, which incorporated the physical notion of quantization first introduced by Planck and the wave like nature of matter hypothesized by de Broglie, was subsequently developed by Schrödinger to treat the electron systems in crystalline materials. The Schrödinger equation for matter waves ψ describes the dynamics of quantum particles. It plays a role of similar importance to that which Newton's equation of motion does for classical particles. As with Newton's laws, the Schrödinger equation cannot be rigorously derived from some underlying, more fundamental principles. Its form can be made plausible, however, by combining the Hamiltonian function of classical mechanics,

$$H=T+V=E \tag{2.13}$$

which equals the mechanical energy, with the de Broglie hypothesis of matter waves

$$\psi(x) =Ae^{i(kx-\omega t)}\ . \tag{2.14}$$

This is further characterized by the wave number $k=2\pi/\lambda=p/\hbar$ and the angular frequency $\omega=2\pi v=E/\hbar$. The ‘‘rationalized’’ Planck's constant $\hbar=h/2\pi=1.05\times10^{-34}\ Js$ is frequently used in quantum mechanics. The physical interpretation of the amplitude A was provided by Born (1926) in terms of a probability density

$$P(x) = |\psi(x)|^2 = |A|^2. \tag{2.15}$$

The potential energy is denoted by V and the kinetic energy by $T = p^2/2m$. Formally multiplying the wave function $\psi(x, t)$ by Eqn. (2.4) yields

$$H\psi(x, t) = [p^2/2m]\, \psi(x, t) + V\, \psi(x, t) \tag{2.16}$$

In order to connect the de Broglie relations for energy and momentum appearing in the arguments of the plane wave (Eqn. 2.14) with the energy and momentum in the Hamiltonian function, H and p in Eqn. (2.16) must be taken as differential operators,

$$\begin{aligned} &H \leftrightarrow i\hbar\, (\partial/\partial t) \\ &p \leftrightarrow (\hbar/i)\, (\partial/\partial x) \end{aligned} \tag{2.17}$$

This substitution into Eqn. (2.13) leads to the time-dependent Schrödinger equation

$$\begin{aligned} i\hbar\frac{\partial}{\partial t} &= H\psi(x,t) \\ &= \left(-\frac{\hbar^2}{2m}\frac{\partial^2}{\partial x^2} + V(x)\right)\psi(x,t) \end{aligned} \tag{2.18}$$

which describes the time evolution of the matter wave. For physical systems that are not explicitly time dependent, i.e., that have time-independent potentials $V(x)$, the energy is conserved and $i\hbar\, (\partial/\partial t)$ can be replaced by E, giving the time-independent Schrödinger equation

$$E\psi(x) = \left(-\frac{\hbar^2}{2m}\frac{\partial^2}{\partial x^2} + V(x)\right)\psi(x)\ . \tag{2.19}$$

If no interaction potential is present ($V(x) = 0$), Eqn. (2.19) is referred to as the *free-particle Schrödinger equation*. The plane waves of Eqn. (2.4) are solutions of the free-particle Schrödinger equation with eigen energies $E = (\hbar k)^2/2m$.

2.11 PERTURBATION THEORY

Atoms are usually studied in the laboratory by applying external fields and observing their effects on the atomic properties. Both magnetic and electric fields alter the atomic spectrum (which may be observed using spectroscopic techniques), and from this one may gain information about the structure of the atom.

In time-independent perturbation theory, there are two levels of the solution - the first is degenerate perturbation theory, and the second non-degenerate theory.

Assume that we have solved the Schrödinger equation for a particular potential with Hamiltonian $H^{(0)}$

$$H^{(0)} \left| n \right\rangle = E_n^{(0)} \left| n \right\rangle \tag{2.20}$$

where $\left| n \right\rangle$ denotes the eigenfunction, and $E_n^{(0)}$ are the eigenvalues. Denote the new Hamiltonian by $H = H^{(0)} + V$, where V is the perturbation. Now if the eigenvalues are non-degenerate, the first order energy correction is given by

$$\Delta E_n^{(1)} \approx \left\langle n \middle| V \middle| n \right\rangle \tag{2.21}$$

and there is no correction in the eigenfunction. This is just the diagonal matrix element of the perturbing potential. The second order correction arises from non-diagonal terms; the energy correction is given by

$$\Delta E_n^{(2)} \approx \sum_{m \neq n} \frac{\left|\langle m|V|n\rangle\right|^2}{E_n^{(0)} - E_m^{(0)}} \tag{2.22}$$

where $|m\rangle$ are all other eigenfunctions. The correction to the eigenfunction is

$$|p\rangle = |n\rangle + \sum_{m \neq n} \frac{\langle m|V|n\rangle}{E_n^{(0)} - E_m^{(0)}} |m\rangle \,. \tag{2.23}$$

Therefore, the total perturbed energy is given by

$$E_n \approx E_n^{(0)} + \Delta E_n^{(1)} + \Delta E_n^{(2)} = E_n^{(0)} + \langle n|V|n\rangle + \sum_{m \neq n} \frac{\left|\langle m|V|n\rangle\right|^2}{E_n^{(0)} - E_m^{(0)}} \tag{2.24}$$

and the perturbed eigenfunction is given by the equation before last.

Some other facts will have a direct impact on band structure calculation by the $\vec{\mathrm{k}}.\vec{\mathrm{p}}$ method. The total second-order perturbation $\Delta E_n^{(2)}$ arises due to the interaction between different eigenvalues. Whether interaction between states occurs or not is determined by the matrix elements $\langle n|V|m\rangle$; if it vanishes, there is no interaction. Whether the states vanish or not can typically be quickly inferred by invoking the symmetry properties of the eigenfunctions and the perturbing potential *V*.

2.12 $\vec{\mathrm{k}}.\vec{\mathrm{p}}$ THEORY

In the $\vec{\mathrm{k}}.\vec{\mathrm{p}}$ method the band structure over the entire Brillouin zone can be extrapolated from the zone centre energy gaps and optical matrix elements. The $\vec{\mathrm{k}}.\vec{\mathrm{p}}$

method is particularly convenient for interpreting optical spectra. In addition, using this method one can obtain analytic expressions for band dispersion and effective masses around high-symmetry points. The $\vec{\mathrm{k}}.\vec{\mathrm{p}}$ method can be derived from the one-electron Schrödinger equation given in Eqn. (2.18). Using the Bloch theorem the solutions of Eqn. (2.16) are expressed, in the reduced zone scheme, as

$$\psi_{nk} = \exp\left(i\vec{k}.\vec{r}\right)u_{nk}\left(\vec{r}\right) \tag{2.25}$$

where n is the band index, **k** lies within the first Brillouin zone, and u_{nk} is periodic in r with the periodicity in Eqn. (2.25) characterized by the wave number k and the energy of a state ψ_{nk} . When ψ_{nk} is substituted into Eqn. (2.19) we can write the equation in $u_{n\boldsymbol{k}}$ of the form

$$\left(\frac{p^2}{2m} + \frac{\hbar\vec{k}.\vec{p}}{m} + \frac{\hbar^2k^2}{2m} + V\right)u_{nk} = E_{nk}u_{nk} \tag{2.26}$$

At $\mathbf{k}_0$ = (0, 0, 0), Eqn. (2.26) reduces to

$$\left(\frac{p^2}{2m} + V\right)u_{n0} = E_{n0}u_{n0} \quad \text{(n= 1, 2, 3 ...)} \tag{2.27}$$

Similar equations can also be obtained for k equal to any point k_0. Eqn.(2.27) is much easier to solve than Eqn. (2.16) since the functions u_{n0} are periodic. The solutions of Eqn. (2.27) form a complete and orthonormal set of basic functions. Once $E_{\boldsymbol{n}\mathbf{0}}$ and $u_{\boldsymbol{n}\mathbf{0}}$ are known, we can treat the terms $\hbar\vec{k}.\vec{p}/m$ and $\hbar^2k^2/(2m)$ as perturbations in Eqn. (2.26) using either degenerate or nondegenerate perturbation theory. This method for calculating the band dispersion is known as the $\vec{k}.\vec{p}$ method. Since the perturbation terms are proportional to k, the method works best for small values of k (Kane, 1966). In general, the method can be applied to calculate the band dispersion near any point $\mathbf{k}_0$ by expanding Eqn. (2.26) around $\mathbf{k}_0$ provided the wave functions (or the matrix elements of

p between these wave functions) and the energies at $\mathbf{k}_0$ are known. Furthermore, by using a sufficiently large number of u_{n0} to approximate a complete set of basic functions, Eqn. (2.26) can be diagonalized with the help of computers to calculate the band structure over the entire Brillouin zone (Wang, 1966). Only a limited number of energy gaps and matrix elements of ***p*** determined experimentally are used as input in the calculation.

2.13 SPIN-ORBIT INTERACTION

Spin-orbit interaction is a well-known phenomenon that manifests itself in lifting the degeneracy of one-electron energy levels in atoms, molecules, and solids. In solid-state physics, the non-relativistic Schrödinger equation is frequently used as a first approximation, e.g. in electron band-structure calculations. Without relativistic corrections, it leads to doubly-degenerated bands, spin-up and spin-down, which can be split by a spin-dependent term in the Hamiltonian. In this approach, spin-orbit interactions can be included as a relativistic correction to the Schrödinger equation.

Kane [1957] calculated the band structure for InSb using the $\vec{k}.\vec{p}$ perturbation approach and assuming that the conduction and valence band extrema are at k = 0. The small band gap requires an accurate treatment of conduction and valence band interactions while higher bands are treated by perturbation theory. Kane noted that the effects of higher and lower bands are treated by perturbation theory. In Kane’s work it enlarges upon the $\vec{k}.\vec{p}$ approach of Dresselhaus [1955] and Parmenter [1955]. The spin-orbit interaction is also treated as a perturbation [Kane, 1956]. Kane assumed that because of the smallness of the energy gap at k = 0 it would be a good approximation to ascribe all of the unusually low effective mass of the conduction band to the mutual interaction of the conduction and valence bands. Kane takes the *k* vector in the z direction and considered the Hamiltonian corresponding to the first four terms of the Schrödinger equation for the cell periodic functions $u_k(r)$

$$\left\{\left(\frac{p^2}{2m}\right)+V+\frac{\hbar}{m}k.p+\left(\frac{\hbar}{4m^2c^2}\right)\left[\nabla V\times p\right].\sigma+\left(\frac{\hbar}{4m^2c^2}\right)\left[\nabla V\times k\right].\sigma\right\}u_k\left(r\right)=E_k^{'}u_k\left(r\right) \qquad (2.28)$$

where $E_k^{'}=E_k-\frac{\hbar^2k^2}{2m}$ and E_k is the energy of a state with wave vector k, and σ represents the Pauli spin matrices

$\sigma_x=\begin{bmatrix}0&1\\1&0\end{bmatrix},\sigma_y=\begin{bmatrix}0&-i\\i&0\end{bmatrix},\sigma_z=\begin{bmatrix}1&0\\0&-1\end{bmatrix}$, given $i=\sqrt{-1}$.

The mutual interaction of the conduction and valence bands leaves the bands doubly degenerate. Kane [1957], takes as a basis $\left|iS\downarrow\right\rangle,\left|\left(X-iY\right)\uparrow/\sqrt{2}\right\rangle,\left|Z\downarrow\right\rangle,\left|\left(X+iY\right)\downarrow/\sqrt{2}\right\rangle$, $\left|iS\uparrow\right\rangle,\left|-\left(X+iY\right)\downarrow/\sqrt{2}\right\rangle,\left|Z\uparrow\right\rangle,\left|\left(X-iY\right)\downarrow/\sqrt{2}\right\rangle$ when he defined the positive constant Δ as the spin-orbit splitting of the valence band which is given by

$$\Delta=\frac{3\hbar \mathrm{i}}{4\mathrm{m}^2\mathrm{c}^2}\left\langle \mathrm{X}\left|\frac{\partial \mathrm{V}}{\partial \mathrm{x}}\mathrm{p}_\mathrm{y}-\frac{\partial \mathrm{V}}{\partial \mathrm{y}}\mathrm{p}_\mathrm{x}\right|\mathrm{Y}\right\rangle. \qquad (2.29)$$

Herman *et al*. (1963) represents the spin-orbit splitting as

$$\Delta=-3\mathrm{i}\left(\frac{\hbar}{4\mathrm{m}_0^2\mathrm{c}^2}\right)\left\langle \mathrm{X}\left|\nabla \mathrm{V}\times \mathrm{p}\right|_\mathrm{y}\mathrm{Z}\right\rangle. \qquad (2.30)$$

and gave the Hamiltonian for the interaction between the spinning and orbital motion of the electrons as

$$H_{spin}=\left(\frac{\hbar}{4m^2c^2}\right)\left[\nabla V\times p\right].\sigma \qquad (2.31)$$

where V *is* the potential energy and the effect of this term may be treated as a perturbation.

2.14 EFFECT OF LARGE MAGNETIC FIELDS

The band structure may be altered by applying an electric field or magnetic field. The electric field causes a shift in the band edge, the magnitude of which is related to the electric field by the relation [Moss, 1961; Franz, 1985; Keldysh, 1985].

$$\Delta E = (3|e|E^{*}\hbar/4\sqrt{2m^{*}})^{2/3} \tag{2.32}$$

where e is the electron charge, E^{*} is a given electric field and m^{*} effective electron mass. This effect is known as Franz-Keldysh effect. Franz-Keldysh calculations show that for the production of a measurable shift (shift in the band edge) a very high value of the electric field is required. The effect is thus observed in few experiments, but there is one example in which the effect is observed in a practical device. The field in the domains of Gunn diodes is often very high, and it has been observed that a light beam may be modulated by the domain field [Guetin and Boccon-Gibod, 1968] through the Franz-Keldysh effect.

2.15 THE DENSITY OF STATES FUNCTION

The density of states for electrons in a band yields the number of states in a certain energy range. This function is important in electronic processes, particularly in transport phenomena. When we denote the density of states function by $g(E)$, it is defined by the relation

$g(E)dE$= number of electron states per unit volume in the energy range $(E,E+dE)$.(2.33)

To evaluate *g(E)* one applies the definition given by Eqn. (2.28). One draws a shell in k-space the inner and outer surface of which are determined by the energy contours *E(k)=E* and *E(k)=E+dE*, respectively, as shown in Figure 2.17. The number of states is then given by the number of allowed *k* values lying inside this shell. When dividing this by the thickness of the shell, *dE*, the desired function *g(E)* is obtained. Clearly from Figure 2.17 that *g(E)* is closely related to the shape of the energy contours, and hence the band structure. The complexities of this structure are reflected in the form taken by *g(E)*.

Electron in the conduction band and holes in the valence band behave as free particles, but their distribution among the available energy levels, when in thermal equilibrium with the lattice, obeys Fermi-Dirac statistics [Fermi, 1926; Dirac, 1926]. The function giving the occupancy of the levels, often called the Fermi function, is [Fermi, 1926]

$$n_s / g_s = 1 / \left\{ 1 + \exp\left[\left(E_s - E_F \right) / k_B T \right] \right\} \tag{2.34}$$

where n_s is the number of electrons occupying levels of energy E_s , the number of which is g_s; k_B is the Boltzman constant, *T* is the temperature, and E_F is referred to as the Fermi energy. The density of states g_s is essentially determined by the E-k relation, whereas E_F is determined by the energy band structure, the doping of the materials, and the operating temperature. The expression for the density of states in the presence of quantizing magnetic field is given as (Nag, 1980)

$$g\ (E)=4\pi(2m^*/h^2)^{3/2}E^{1/2}\ . \tag{2.35}$$

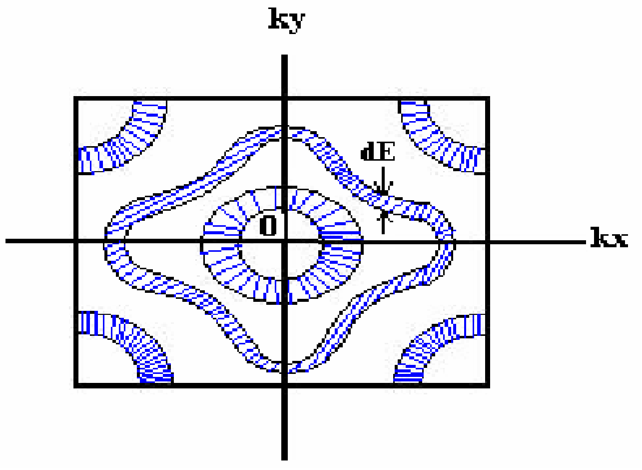

Figure 2.17: Concentric shells in k-space used to evaluate the DOS, g(E) [Erkoç and Uzer, 1996].

2.16 DENSITY FUNCTIONAL THEORY FROM WAVE FUNCTIONS TO ELECTRON DENSITY

The density functional theory is one of the attractive theoretical methods to study the structural and electronic properties of solids. The two fundamental mathematical theorems proved by Hohenberg and Kohn [1964] and the derivations by Kohn and Sham [1965] in the mid-1960 are important for the entire field of DFT. In the Hohenberg and Kohn theory, the DFT is stated by two theorems. The first demonstrates a uniqueness of the ground state energy which is a function of the electron density from Schrödinger equation. The second H-K theorem proves that the true electron density corresponding to the full solution of the Schrödinger equation is the electron density that minimizes the energy of the overall functional. The H-K theorem describes a function that is useful to write in terms of the single-electron wave function, $\psi(r)$

$$E\left[\{\psi\}\right]=E_{known}\left[\{\psi\}\right]+E_{xc}\left[\{\psi\}\right] \tag{2.36}$$

$$E_{known}\left[\{\psi\}\right]=-\frac{\hbar^2}{2m}\sum\int\psi^*\nabla^2\psi d^3r+\int V(r)n(r)d^3r+\frac{e^2}{2}\iint\frac{n(r)n(r')}{|r-r'|}d^3rd^3r'+E_{ion} \tag{2.37}$$

From Eqn. (2.36), the energy function can be expressed as a split of a simple analytical form, $E_{known}[\{\psi\}]$ and all the quantum mechanical effects that are not included in the "known" terms is defined as the exchange-correlation functional $E_{xc}[\{\psi\}]$. The "known" terms include four contributions that are shown in Eqn. (2.37). The terms on the right are, in order, the electron kinetic energies, the Coulomb interactions between electrons and nuclei, the Coulomb interactions between pairs of electrons, and the Coulomb interactions between pairs of nuclei. The difficulty in fully solving the Schrödinger equation is eliminated by using the Kohn and Sham [K-S] equation, which only involves a single electron. In K-S formulation, Eqn. (2.37), energy is calculated by solving a series of one-electron equations of the form

$$\left[-\frac{\hbar^2}{2m}\nabla^2+V(r)+V_H(r)+V_{xc}(r)\right]\psi(r)=\varepsilon\psi(r) \tag{2.38}$$

These equations are quite similar to the Schrödinger equation, Eqn. (2.16).The first term on the left-hand side describes the kinetic energy of the electron, V is the potential energy of an electron interacting with the nuclei, V_H is the Hartree potential and V_{xc} is the exchange-correlation potential. The Hartree potential is expressed as

$$V_H(r)=e^2\int\frac{n(r)}{|r-r'|}d^3r' \tag{2.39}$$

describes the Coulomb repulsion between the electron and the total electron density of the system. The energy V_{xc} which defines exchange and correlation contributions to the single-electron is written as

$$V_{xc}(r)=\frac{\delta E_{xc}(r)}{\delta n(r)} \tag{2.40}$$

The "functional derivative" is written using δ rather d to emphasize that it is not a normal derivative. The exchange-correlation potential at the electron density observed at that position is

$$V_{xc}\left(r\right)=V_{xc}^{electrongas}\left[n\left(r\right)\right] \qquad (2.41)$$

where *n(r)* is the electron density, and in the case of uniform electron gas the electron density is constant at all points in space.

2.16.1 Local-Density Approximation (LDA)

The oldest, simplest and probably the most important function is the local density approximation (LDA), which was proposed by Hohenberg and Kohn [1964] in their original DFT paper. The LDA consists of locally approximating the true exchange-correlation energy of a system by the exchange-correlation energy associated with a homogeneous electron gas of the same density. The homogeneous gas is the only system for which the form of the exchange-correlation energy is known precisely. The LDA is only dependent on the local density, and the total energy is commonly written as

$$E_{xc}^{LDA}\left[n\left(\vec{r}\right)\right]=\int d^3\vec{r}\, n\left(\vec{r}\right)\varepsilon_{xc}\left[n\left(\vec{r}\right)\right] \qquad (2.42)$$

where $\varepsilon_{xc}\left[n\left(\vec{r}\right)\right]$ is the exchange-correlation energy density corresponding to a homogeneous electron gas of density $n\left(\vec{r}\right)$.

A symbolic graphical description of the local character of LDA approximation is shown in Figure 2.18.

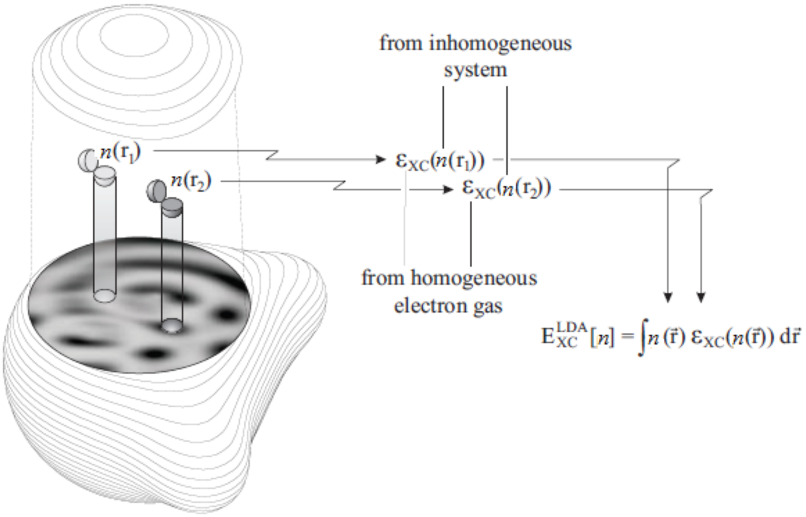

Figure 2.18: The local density approximation [Koch and Holthausen, 2001].

2.16.2 Local-Spin-Density Approximation (LSDA)

The extension of LDA function to spin-polarized systems is important especially for correct description of elements subjected to magnetism. The formulation is straightforward for exchange energy part, where the exact spin-scaling is known, but for correlation energy term further approximations must be employed.

A spin polarized system in DFT employs two spin-densities n_α and n_β with the total $n = n_\alpha + n_\beta$, and the form of the *local-spin-density approximation (LSDA)* (Von Barth and Hedin, 1972) is as follows:

$$E_{xc}^{LSDA}\left[n_\alpha(\vec{r}), n_\beta(\vec{r})\right] = \int d^3\vec{r}\, n(\vec{r})\, \varepsilon_{xc}\left[n_\alpha(\vec{r}), n_\beta(\vec{r})\right] \qquad (2.43)$$

For the exchange energy, the exact result (not just for local density approximation) is known in terms of the spin-unpolarized function [Oliver and Perdew, 1979]:

$$E_x\left[n_\alpha, n_\beta\right] = \frac{1}{2}\left(E_x\left[2n_\alpha\right] + E_x\left[2n_\beta\right]\right) \qquad (2.44)$$

The spin-dependence of the correlation energy density is approached by introducing the relative spin-polarization:

$$\zeta(r) = \frac{n_\alpha(\vec{r}) - n_\beta(\vec{r})}{n_\alpha(\vec{r}) + n_\beta(\vec{r})} \qquad (2.45)$$

A value of $\zeta = 0$ corresponds to the paramagnetic spin-unpolarized situation with equal α, and β, spin densities, whereas $\zeta = \pm 1$ corresponds to the ferromagnetic (fully polarized) situation where one spin density vanishes. The spin correlation energy density for a given value of the total density and relative polarization, $\varepsilon_C(n, \zeta)$, is constructed so to interpolate the extreme values. Several forms have been developed in conjunction with LDA correlation function [Oliver and Perdew, 1979; Vosko *et al.*, 1980].

2.16.3 Generalized Gradient Approximation (GGA)

Hohenberg and Kohn presumed that the LDA would be too simple to work for real systems and so proposed an extension to the LDA known as the gradient expansion approximation (GEA) [Hohenberg and Kohn, 1964]. The GEA is a series expansion of increasingly higher order density gradient terms. The first order form of the GEA was subsequently implemented and tested for atoms and molecules and was a complete failure. Anyway, GEA provided the basis for the generalized gradient approximation (GGA), which is currently the most used exchange-correlation function in computational material physics.

The vital steps that lead to the GGA were principally made by Perdew [1985] who devised a cutoff procedure that sharply terminates the GEA exchange-correlation hole in real-space using delta functions, in order to restore the sum rule and non-positive hole conditions. As a result of this procedure the GGA can be conveniently written in terms of an analytic function known as the enhancement factor, $F_{xc}\left[n(\vec{r}),\nabla n(\vec{r})\right]$, that directly modifies the LDA energy density,

$$E_{xc}^{GGA}\left[n(\vec{r})\right]=\int d^3\vec{r}\,n(\vec{r})\,\varepsilon_{xc}^{\hom}\left(n(\vec{r})\right)F_{xc}\left[n(\vec{r}),\nabla n(\vec{r})\right] \qquad (2.46)$$

Using GGA, very good results for molecular geometries and ground-state energies have been achieved.

2.17 CAMBRIDGE SERIAL TOTAL ENERGY PACKAGE (CASTEP)

CASTEP [Clark et al., 2005] is a state-of-art quantum mechanics-based program designed specifically for solid-state materials science. CASTEP employs the DFT plane-wave pseudopotential method, which allows to perform first-principles quantum mechanics calculation that explore the properties of crystals and surfaces in materials such as semiconductors, ceramics, metals, mineral and zeolites. The CASTEP uses the pseudopotentials and the general overview of density functional theory provides information on the concepts of charge density, DFT functional, the self-consistent field (SFT) procedure and band structure, which are applicable to any computation of DFT.

CASTEP requires that all studies must be performed on a periodic system. In a periodic system each electronic wave function can be written as a product of a cell-periodic part and a wavelike part [Payne et al., 1992] is the main advantage of imposing periodic boundary conditions related to Bloch's theorem, Eqn. (2.4). Of a discrete set of plane waves, consisting of a basis set, is used for expanding the cell periodic part, ψ whose wave vectors are reciprocal lattice vectors of the crystal as shown in Eqn. (2.47)

$$\psi_i(r) = \sum_G C_{i,G} e^{iG.r} \tag{2.47}$$

where the reciprocal lattice vectors G are defined by G.*l*=2*πm* for all *l* where *l* is a lattice vector of the crystal and *m* in an integer. Therefore, each electronic function can be written as a sum of plane waves,

$$\psi_i(r) = \sum_G c_{i,k+G} e^{iG.r} \tag{2.48}$$

2.17.1 Exchange-Correlation Function

A number of exchange-correlation functional such as local (LDA), gradient-corrected (GGA), and fully nonlocal are implemented in CASTEP. The exchange-correlation for LDA functional is same as in Eqn.(2.41). The Perdew and Zunger [Perdew and Zunger, 1981] parameterization of the numerical results of Ceperley and Alder [Ceperley and Alder, 1980], CA-PZ is the only one local function provided in CASTEP. The consideration of the local representation of the exchange-correlation potential in this particular prescription is to be one of the most accurate descriptions available [Srivastava and Weaire, 1987]. The *dn/dr* as well as *n* is dependent on the so-called nonlocal or gradient-corrected function. The gradient corrected calculation provides a considerable increase in the accuracy of predicted energies and structures. The Perdew-Wang generalized-gradient approximation (PW91) and Perdew-Burke-

Ernzerhof correlations (PBE) are also useful for improving the accuracy of the calculation.

2.17.2 Pseudopotential

Since the full Coulomb potential of the electron-ion interaction decays too slowly to be accurately presented by a small number of Fourier components, the concept of pseudopotential has been treated on each atom in the CASTEP. The degree of hardness of pseudopotential is an important concept in the pseudopotential applications and is considered as soft when a small number of Fourier components is required for its accurate representation and it is hard otherwise.

The potentials for transition metals and for first row elements (O, C, N, etc.) turn out to be extremely hard [Bachelet et al., 1982; Kerker, 1980] are quickly showed in the early development of accurate norm-conserving pseudopotentials. Various values of pseudopotentials have been suggested to improve. The improvement of convergence properties of norm-conserving pseudopotentials (Troullier and Martins, 1991) has been suggested by various schemes. The kinetic energy optimization scheme developed by Lin *et al.* (1993) and Lee (1996) are used to generate norm-conserving potentials in CASTEP.

2.17.3 Self-consistent Electron Minimization

A choice of methods for electronic relaxation is offered by CASTEP and the default is the most efficient and is based on density mixing [Kresse et al., 1996]. In this scheme, instead of the self-consistent minimization of the total energy, the sum of electronic eigenvalues is minimized in the fixed potential. At the end of the minimization the new charge density is mixed with the initial density and the process is repeated until convergence is reached. The sum of eigenvalues is minimized using the conjugate gradient-based approach.

A more traditional scheme for electronic relaxation is supported by CASTEP involving minimization of the total energy. A plane-wave basis set is used to expand the electronic wave functions and varied so as to minimize the total energy. An all-bands method performed the minimization that allows simultaneous update of all wave functions. A preconditioned conjugate gradients technique [Payne et al., 1992] is used for this scheme.

2.18 SUMMARY

The band structure of a material determines several characteristics, in particular the material's electronic and optical properties. Bands have different widths, depending upon the properties of the atomic orbital and the difference in the type of solids may be attributed to the band gap. The atoms in crystals are arranged in a periodic potential which gives the energy bands. A semiconductor is a material with a small but nonzero band gap. The conductivity of intrinsic semiconductors is strongly dependent on the band gap. The band gap energy of semiconductors tends to decreasing with increasing temperature as shown in Eqn. (2.1)

$$Eg\left(T\right)=Eg\left(0\right)-\frac{\alpha T^{2}}{T+\beta}$$

which is known as Varshni's empirical expression. The crystal is characterized to be a semiconductor if one or two conduction bands are slightly filled or slightly empty. The conductivity dependence on temperature of a material is the property that enables semiconductors to conduct current since the conductivity and intrinsic carrier concentration are largely controlled by Eg/k_BT, the ratio of the band gap to thermal energies.

Ghatak *et al.*, [2008] expressed the band gap of semiconductors by the expression given in Eqn. (2.2)

$$Eg = Eg_0\left(1+\left(\frac{2m_c}{\mu^*}\right)\frac{E\left(1+\alpha E\right)}{Eg_0}\right)^{\frac{1}{2}}$$

where m_c is the effective electron mass at the edge of the conduction band, and μ^* is the reduced mass which is given by

$$\frac{1}{\mu^*}=\frac{1}{m_c}+\frac{1}{m_v}$$

m_v is the effective mass of the heavy hole at the top of the valence band , Eg_0 is the unperturbed band gap, and $\alpha=1/Eg_0$. Ghatak *et al.*, [2008] studied the Boltzmann transport equation on the basis of this equation and have introduced new physical ideas experiments in the presence of external photo excitation.

For ZnS_xSe_{1-x} $(0\leq x\leq 1)$ as II-VI Compounds there are two possible structures can be formed from such tetrahedral: the sphalerite (cubic type) and the wurtzite (hexagonal) type. The sphalerite structure is very similar to the structure of diamond, but it differs from the latter by the alternation of atoms of two different elements.

The density functional theory is one of the attractive theoretical methods to study the structural and electronic properties of solids. Local-density approximations (LDA) are a class of approximations to the exchange-correlation (XC) energy functional in density functional theory (DFT) that depend solely upon the value of the electronic density at each point in space. Many approaches can yield local approximations to the

XC energy. However, overwhelmingly successful local approximations are those that have been derived from the homogeneous electron gas (HEG) model. In this regard, LDA is generally synonymous with functional based on the HEG approximation, which are then applied to realistic systems (molecules and solids). For a spin-unpolarized system, a local-density approximation for the exchange-correlation energy is written as Eqn. (2.42)

$$E_{xc}^{LDA}\left[n\left(\vec{r}\right)\right]=\int d^{3}\vec{r}\,n\left(\vec{r}\right)\varepsilon_{xc}\left[n\left(\vec{r}\right)\right]$$

where $n(\vec{r})$ is the electronic density and $\varepsilon_{\mathrm{xc}}$, the exchange-correlation energy density, is a function of the density alone. The exchange-correlation energy is decomposed into exchange and correlation terms linearly,

$$E_{xc}=E_{x}+E_{c}.$$

CASTEP is a state-of-art quantum mechanics-based program designed specifically for solid-state materials science. The CASTEP uses the pseudopotentials and the general overview of density functional theory provides information on the concepts of charge density, DFT functional, the self-consistent field (SFT) procedure and band structure, which are applicable to any computation of DFT.